

Quantitative comparison of lung physiological parameters in single and multiple breathhold with hyperpolarized xenon magnetic resonance

This content has been downloaded from IOPscience. Please scroll down to see the full text.

2016 Biomed. Phys. Eng. Express 2 055013

(<http://iopscience.iop.org/2057-1976/2/5/055013>)

View [the table of contents for this issue](#), or go to the [journal homepage](#) for more

Download details:

IP Address: 202.127.153.14

This content was downloaded on 22/09/2016 at 02:11

Please note that [terms and conditions apply](#).

Biomedical Physics & Engineering Express



PAPER

Quantitative comparison of lung physiological parameters in single and multiple breathhold with hyperpolarized xenon magnetic resonance

RECEIVED
27 March 2016

REVISED
4 August 2016

ACCEPTED FOR PUBLICATION
9 August 2016

PUBLISHED
21 September 2016

Zhiying Zhang^{1,3}, Yu Guan^{2,3}, Haidong Li¹, Xiuchao Zhao¹, Yeqing Han¹, Yi Xia², Xianping Sun¹, Shiyuan Liu², Chaohui Ye¹ and Xin Zhou¹

¹ Key Laboratory of Magnetic Resonance in Biological Systems, State Key Laboratory of Magnetic Resonance and Atomic and Molecular Physics, National Center for Magnetic Resonance in Wuhan, Wuhan Institute of Physics and Mathematics, Chinese Academy of Sciences, Wuhan 430071, People's Republic of China

² Department of Radiology, Changzheng Hospital of the Second Military Medical University, Shanghai 200003, People's Republic of China

³ These authors contributed equally to this work.

E-mail: xinzhou@wipm.ac.cn

Keywords: hyperpolarized gas imaging, MRI, ¹²⁹Xe, lung, chemical shift saturation recovery

Abstract

Hyperpolarized (HP) xenon MR has been an important tool for quantifying the pulmonary structure and gaining functional information by measuring the dynamics of xenon in different lung components, e.g., gas exchange between gaseous xenon in the alveoli and dissolved xenon in tissue/plasma and red blood cells. Chemical shift saturation recovery is a commonly used pulse sequence to measure the xenon dynamics in the lung globally. However, the effect of the dissolved xenon signal oscillation caused by the cardiac cycle on the physiological parameters of the lung is still unclear. In this study, both single-breathhold (SB) and multiple-breathhold (MB) measurements were used to evaluate these effects in rats, and the data acquired with the MB measurement, which did not have oscillations, served as a reference. The pulmonary physiological parameters were extracted using the model of xenon exchange. The results showed that the physiological parameters derived from SB and MB measurements were not significantly different. These findings have clarified a previously unknown issue and will further promote the design of faster real-time acquisition sequences to quantify structural and functional information about the lung.

1. Introduction

Chest x-rays and computer tomography (CT) are the routine clinical imaging modalities for pulmonary disease diagnosis. However, these methods have a risk of cumulative radiation doses and cannot visualize and quantify pulmonary gas exchange functions (Sodickson *et al* 2009). Hyperpolarized noble gas MR, which does not employ ionizing radiation and has an extremely high MR signal sensitivity, has been demonstrated to have great potential for the evaluation of the lung structure and to provide functional information since its first application in an excised mouse lung (Sakai *et al* 1996, Driehuys *et al* 2006, Mugler *et al* 2010, Dregely *et al* 2012, Marshall *et al* 2014). Among the commonly used noble gas isotopes (³He, ⁸³Kr and ¹²⁹Xe), hyperpolarized xenon MR has an exclusive advantage of quantitatively providing

structural and functional information about the lung due to its high lipid solubility and high sensitivity to chemical shifts in the adjacent environment. Therefore, it has been widely used to quantify pulmonary physiological parameters in both animals and humans (Ladefoged and Andersen 1967, Peterson *et al* 2011, Driehuys *et al* 2012, Mugler and Altes 2013).

Generally, pulmonary gas exchange functions have been quantified via the dynamics of dissolved xenon in the lung. Xenon polarization transfer contrast (XTC) and chemical shift saturation recovery (CSSR) are the methods currently used to determine the dynamics of dissolved xenon in the lung (Ruppert *et al* 2000, Patz *et al* 2008, Driehuys *et al* 2009, Patz *et al* 2011, Cleveland *et al* 2012). XTC proposed by Ruppert and colleagues, determines the dynamics of dissolved xenon by measuring the decrease in the gas-phase xenon signal after saturating the dissolved

xenon signals (i.e., xenon in red blood cells (RBC) and in tissue and plasma (TP)). By taking advantage of the strong xenon signal in the gas phase, XTC can provide spatially resolved measurements of pulmonary function via hyperpolarized xenon depolarization maps (Ruppert *et al* 2000). In addition, some physiological parameters such as the alveolar-volume ratio, the alveolar septum thickness, etc, can be obtained by using the multiple exchange time xenon polarization transfer contrast technique (MXTC) (Dregely *et al* 2011, Muradyan *et al* 2013). However, in XTC, the dissolved xenon signals from the RBC and the TP are treated as a single signal and cannot be distinguished. The other method, CSSR, directly measures the dissolved xenon signal in the RBC and the TP, and the dynamics of the xenon signal in the RBC and the TP can be simultaneously obtained as a function of the exchange time (i.e., the time between the saturation pulse and the excitation pulse). CSSR has shown great potential for investigating the pulmonary microstructure and function *in vivo* by acquiring the dynamics of dissolved xenon and has been widely used in preliminary studies to quantify the physiological changes caused by lung disease in both animals and humans (Patz *et al* 2008, 2011).

Pulmonary physiological parameters can be extracted from CSSR data by using gas exchange models. The Månsson model, the Patz model and the model of xenon exchange (MOXE) are the most widely used gas exchange models (Månsson *et al* 2003, Patz *et al* 2011, Chang 2013, Fox *et al* 2014). The physiological parameters extracted from all models correlate with each other to the significance level of $P < 0.01$ (Stewart *et al* 2014). In MOXE, the xenon signals from the TP and RBCs are treated individually and the effect of the blood flow is also considered (Chang 2013). Accordingly, the model is more realistic, and more comprehensive physiological parameters of the lung can be obtained such as the gas exchange time constant. MOXE is a major improvement in the theories and models for analyzing pulmonary function parameters based on CSSR data, although the fitting is much more complicated.

Generally, two acquisition modes are utilized in CSSR data collection according to the average time, as shown in figure 1. One mode is multiple-breathhold (MB) measurement in which each data point of the CSSR is acquired in a single breath with averaging (Chen *et al* 2003, Driehuys *et al* 2006, Imai *et al* 2010). The other is single-breathhold (SB) measurement in which all of the data are collected in the same breathhold without averaging. This mode is commonly used in human experiments (Abdeen *et al* 2006, Patz *et al* 2008, Qing *et al* 2014). MB measurement has generally been used in animal experiments to improve the SNR of the dissolved xenon signal to reduce the fitting error. It is necessary to mention that MB measurement could also average out the fluctuation caused by pulsatile blood flow. Averaging SB measurements has

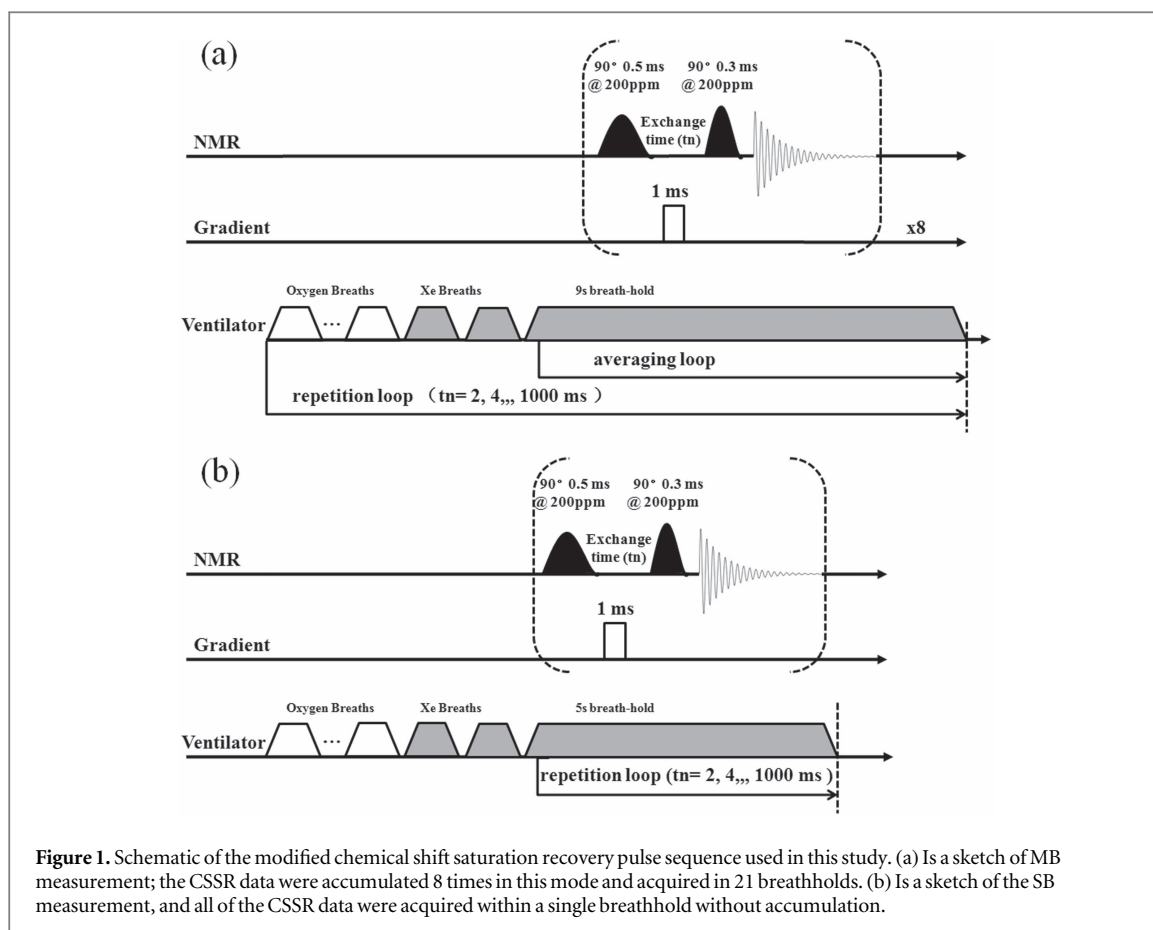
recently been proposed in some studies (Stewart *et al* 2014). Mugler and colleagues recently found that the dissolved ^{129}Xe spectra in the lung are sensitive to the pulmonary circulation caused by the cardiac cycle, and the oscillation of the xenon signal from RBCs could be as large as 15% (Ruppert *et al* 2015, Norquay *et al* 2016). These findings indicated that the physiological parameters extracted from CSSR data via the gas exchange model may be affected by the oscillation of the RBC xenon signal. Measurement of the actual pulmonary physiological parameters, which reflect the biological and pathological functions, is very crucial for the early detection and diagnosis of pulmonary disease.

In this study, the effects of the RBC xenon signal oscillation on the fitting results from the CSSR data via MOXE were quantitatively evaluated. Two acquisition modes, single-breath and multiple-breath acquisitions, were utilized to evaluate the effect, and the multiple acquisition was intended to serve as reference data without the oscillation effect. In multiple-breath acquisitions, the data were acquired with a repetition time that is incommensurate with the heart rate, in order to average out the pulsatile effect from the blood flow. The main physiological parameters extracted from the CSSR data via MOXE were analyzed, and no significant differences were found between the acquisition modes.

2. Material and method

2.1. Xenon polarizer and hyperpolarized ^{129}Xe gas preparation

The nuclear spin of ^{129}Xe was polarized using a polarizer built in our laboratory via the collisional spin exchange with optically pumped rubidium vapor (Zhou 2011). The polarizer was equipped with a 75 W laser diode array system of narrowed line-width (QPC Lasers, Sylmar, CA) that worked in flow-through mode. The gas mixture, which was composed of 1% enriched xenon (85% ^{129}Xe), 10% nitrogen and 89% helium, flowed through the optical cell filled with approximately 1 gram of rubidium at 0.4 standard litres per minute (SLPM) with a pressure of 4 bar in the opposite direction of the laser beam. After polarization, the spin polarization of ^{129}Xe was approximately 20%. Then, the gas mixture was passed through a cold finger, which was placed in a magnet with a field of approximately 200 mT and immersed in liquid nitrogen. Xenon was trapped in its solid state, while nitrogen and helium flowed through because of their lower melting points. Hyperpolarized xenon was accumulated for approximately one hour in each experiment. Then, the hyperpolarized xenon was transferred to a Tedlar bag after thawing into gas with hot water. The available spin polarization of the hyperpolarized xenon gas in the Tedlar bag was approximately 10%.



2.2. Hyperpolarized xenon gas delivery

Hyperpolarized xenon gas was delivered to the rat lung by using an MRI-compatible delivery system built in our laboratory. By using a series of non-magnetic pneumatic valves controlled by a LabVIEW program, the delivery system delivered a precise volume of gas to the rat's lungs. The tube and pneumatic valve HP gas pass-through must be constructed from nondepolarizing materials to protect the polarization. Additionally, the inspiration, breath-holding and expiration time can be adjusted according to experimental requirements. The delivery system could also monitor the pressure in the rat lung in real time and trigger the MRI scanner to start acquisition.

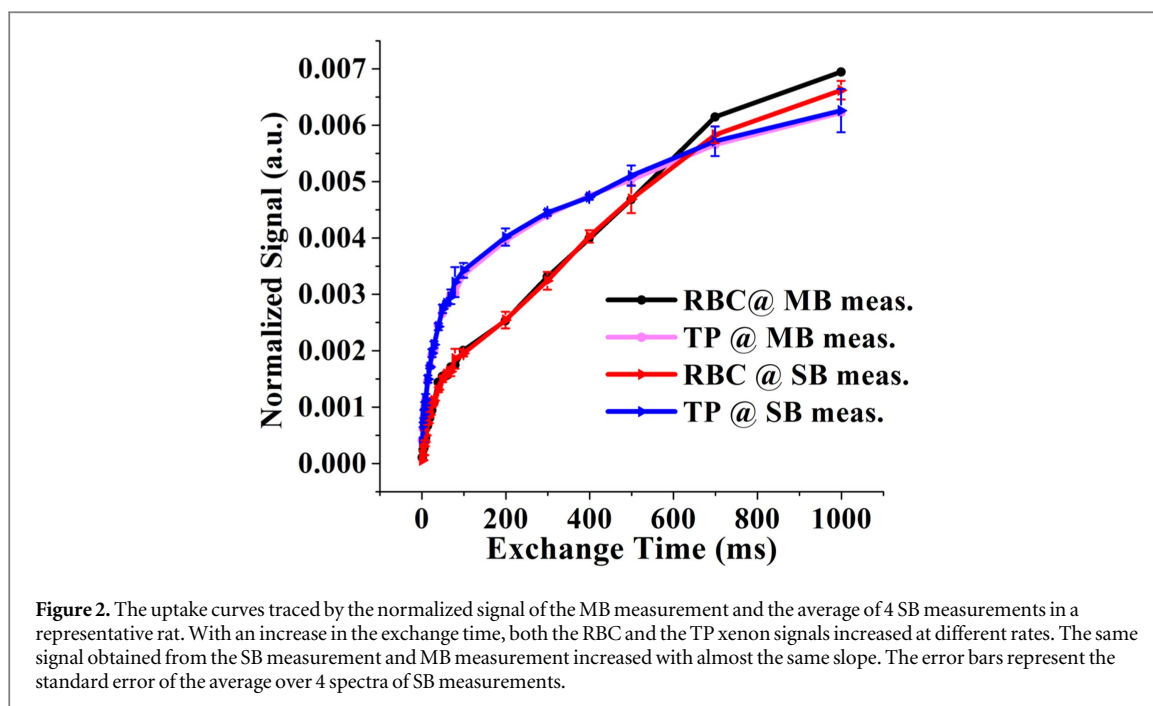
2.3. Animal preparation

All animal handling protocols were approved by the institutional animal care committee. Six healthy Wistar rats weighing 200 ± 20 g were used in this study. A 2 mm catheter was utilized to alternately ventilate the rats with hyperpolarized xenon and oxygen gas. Anaesthesia was induced with 5% isoflurane in 95% oxygen, and 1.5% isoflurane with balanced oxygen was used to maintain anaesthesia during the experiments. The rats were attached to the ventilation tube through tracheal intubation (Nouls *et al* 2011). The rats were ventilated in the prone position at a rate of 60 breaths/min with a tidal volume of 3 ml. The experimental rats were exposed to cigarette smoke

twice a day for 5 days per week. The exposure was about 30 min each time and continued for 6 months to establish a cigarette smoke injury model (Zhu *et al* 2012). A comparison between healthy and exposed rats was done to test whether the two acquisition methods could distinguish functional alterations in the exposed rats and both methods worked well. At the end of the experiments, the rats were sacrificed by means of an intraperitoneal injection of sodium pentobarbital (200 mg kg^{-1}), and the lungs were extracted and immersed in 4% paraformaldehyde liquid for more than 48 h before embedding in paraffin. Hematoxylin and eosin-stained histological slice sections were assessed according to the standard protocol (Li *et al* 2015).

2.4. Hyperpolarized xenon MR spectroscopy

All of the experiments were conducted on a Bruker Biospec 4.7 T animal MRI scanner. A $^1\text{H}/^{129}\text{Xe}$ dual-tuned birdcage coil built in our laboratory with a diameter of 55 mm and length of 240 mm was used for data collection. The ^1H (200.29 MHz @ 4.7 T) channel was used to locate the position of a rat in the scanner, in order to place the rat's lung in the center of the magnet. The ^{129}Xe (55.4 MHz @ 4.7 T) channel was intended to acquire the hyperpolarized ^{129}Xe lung signal. The pulse sequence used for the CSSR data collection has been described in a previous study (Li *et al* 2015). Following a Gaussian-shaped RF saturation



pulse centered at 200 ppm (the gas phase was 0 ppm) for saturating the dissolved xenon signals, a Gaussian-shaped RF excitation pulse was applied for data collection, as shown in figure 1. By changing the exchange time (t_n), i.e., the time between the saturation and excitation RF pulses, the dynamics of the dissolved xenon in the lung can be obtained. The exchange time was increased from 2 to 1000 ms (i.e., 2, 4, 6, 8, 10, 15, 20, 25, 30, 40, 50, 60, 70, 80, 100, 200, 300, 400, 500, 700, and 1000 ms). The acquisition bandwidth was 25 KHz, and the number of sampled points was 1024. Before acquisition, the rat lung was flushed with xenon twice in order to improve the SNR of the dissolved xenon. For each rat, four sets of data from the SB measurement and a dataset from the MB measurement were collected. For the SB measurement, all of the CSSR data were acquired successively from short exchange time to long exchange time in one breathhold without averaging, and the acquisition was repeated 4 times to measure its reliability. For the MB measurement, the data were acquired in one breathhold at the various exchange times with an average of 8, and 21 breathholds were included.

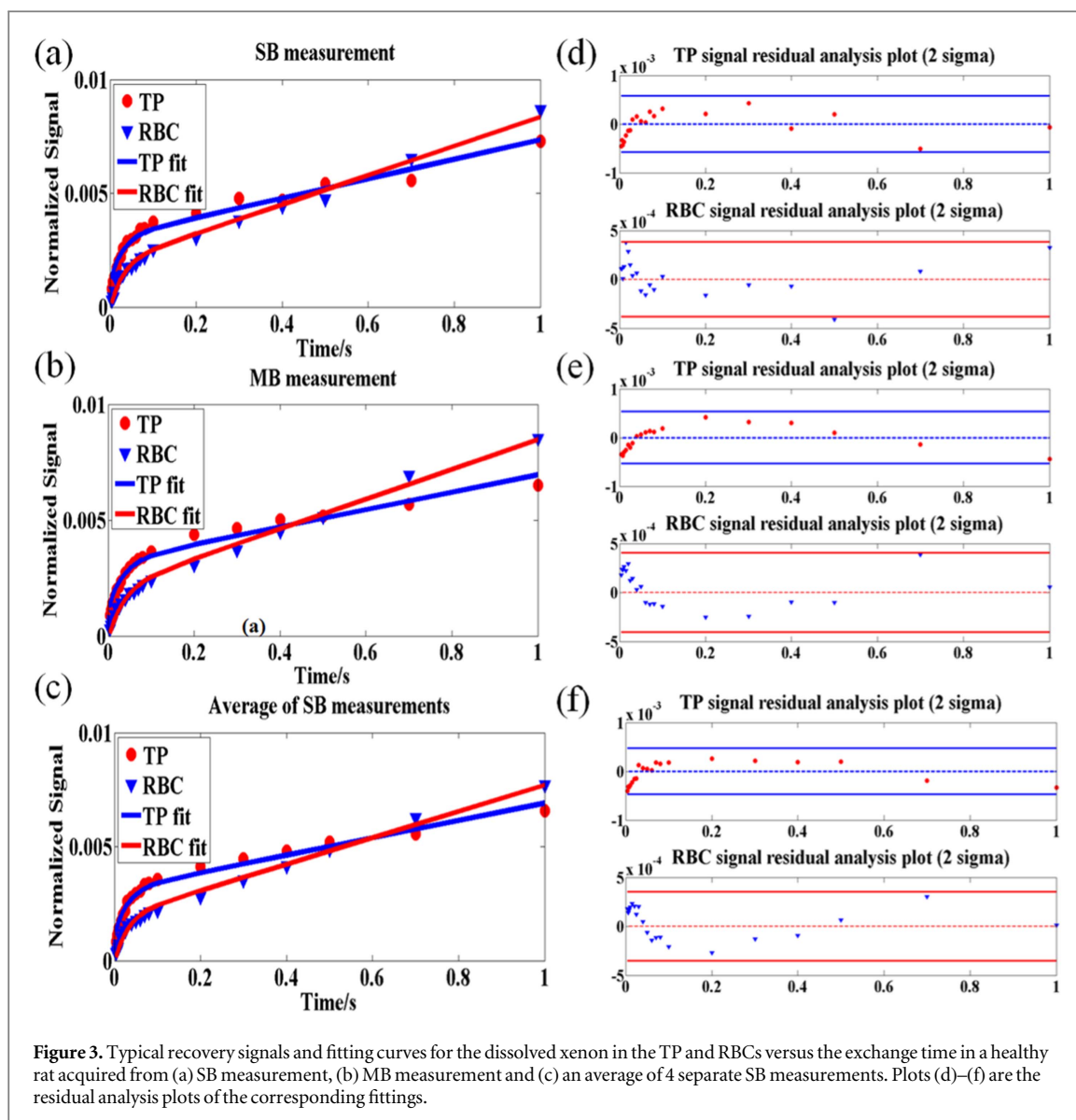
All of the spectra were processed in the Topspin 3.0. Before Fourier transformation, a 50 Hz exponential line-broadening filter was applied to improve the SNR. The amplitudes of the RBCs and TP were extracted by fitting the spectra using the Lorentzian shape function after phase calibration. The RBCs and TP signals were normalized with the corresponding gas peak for fitting to MOXE. Finally, the signals obtained from the RBCs and TP ($S_{RBC}(t)$ and $S_{TP}(t)$) were simultaneously fitted in Matlab, and the pulmonary physiological parameters, including the barrier-to-septum ratio (δ/d), the gas exchange time constant (T), the surface area to volume ratio (SVR), the septal wall

thickness (d), the pulmonary transit time (t_x), etc, could be extracted. In the SB method, each set of data was analysed using MOXE model without averaging. The fitting details were as described in a previous study (Li *et al* 2015).

3. Results

The representative hyperpolarized ^{129}Xe uptake curves traced by the normalized signal of MB measurement and the average of 4 SB measurements are shown in figure 2. The typical dynamics acquired from SB and MB measurements in the representative lung are shown in figure 3. The xenon signals from the RBCs and TP had a similar trend in both acquisition modes. Both the TP and the RBC xenon signals increased with an increasing exchange time, and the RBC xenon signal was lower than the TP xenon signal when the exchange time was short. However, when the exchange time was longer than 500 ms, the RBC xenon signal was generally higher than the TP xenon signal. Figures 3(a)–(c) shows the representative replenishment and fitting curve for the SB measurement, the MB measurement and the average of 4 SB measurements. Figures 3(d)–(f) is residual plots of three different conditions. The fitting results were consistent with each other, and the fitting degree was very good. The residual errors were all within 2σ .

The mean values and standard deviation of eight parameters extracted from the two different acquisition modes are shown in table 1. The difference between the parameters extracted from MOXE by using the data acquired from both acquisition modes was less than 5%, which suggested good consistency between the different modes. Parameters derived from



the SB measurement and multiple acquisitions were correlated at a significance level of $P < 0.01$. The reliability was evaluated by Cronbach's α coefficients and the intraclass correlation coefficient. Both the Cronbach's α coefficients and the intraclass correlation coefficient showed good internal consistency and reliability between the different modes, and the measured Cronbach's α coefficients and the intraclass correlation coefficient were more than 0.85 and 0.75, respectively. To validate an agreement between the two different measurement modes, Bland–Altman plots of the exchange time constant (T), the pulmonary capillary transit time (tx), the total septal thickness (d) and the air–blood barrier thickness (δ) were also analysed, as shown in figure 4.

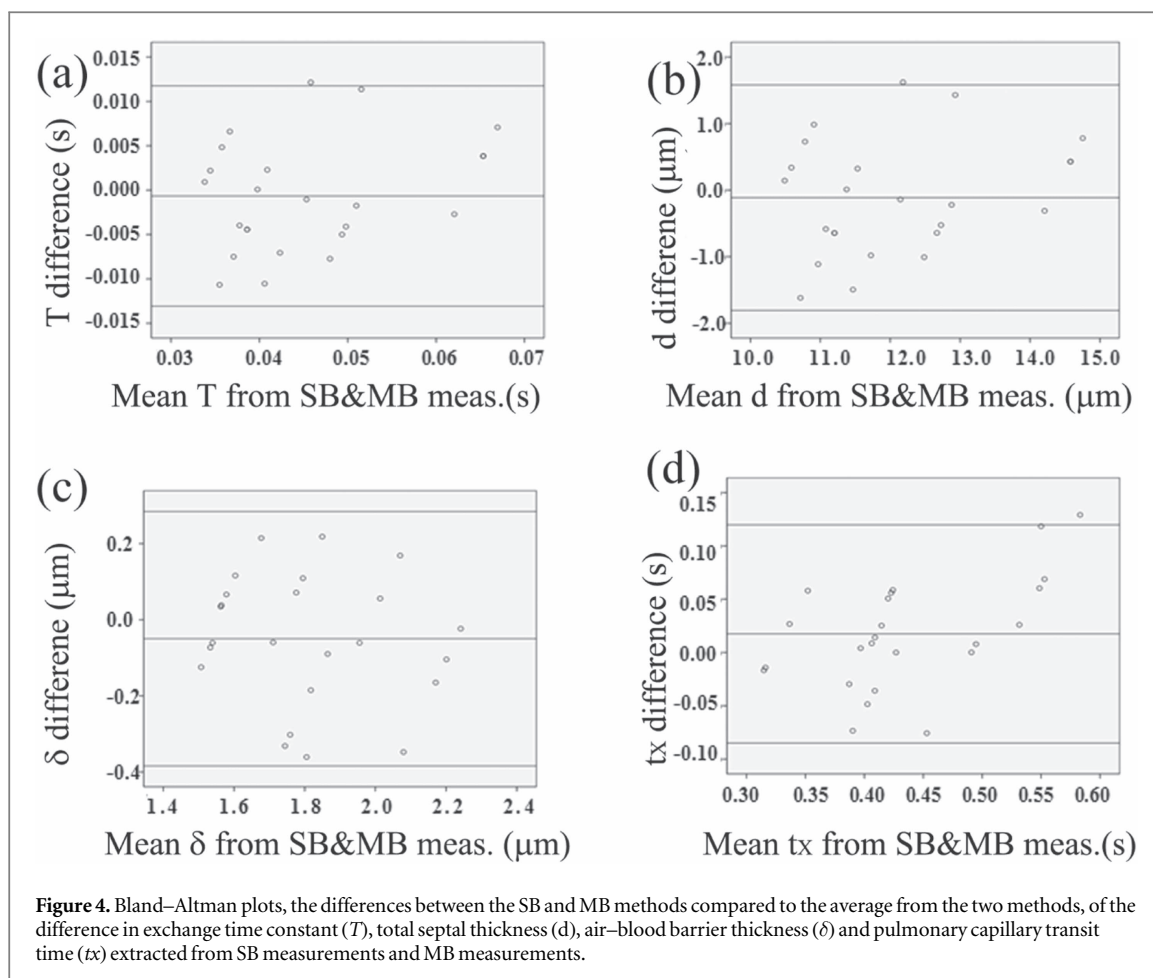
To verify the feasibility of the SB measurement mode for evaluating the changes in the microstructure and gas exchange function caused by disease in rat lung, two rats with COPD induced by passive smoking were assessed with both modes. For the SB measurement, the refreshed CSSR signal was acquired 4 times

for each rat. Therefore, three sets of MOXE fitting results could be obtained from the SB measurement data, the MB measurement data and the average of 4 SB measurement data. The exchange time constants extracted from the SB measurement, the MB measurement and the average of the SB measurements were 0.05 ± 0.01 s, 0.05 ± 0.01 s, and 0.04 ± 0.01 s for healthy rats and 0.08 ± 0.02 s, 0.08 ± 0.01 s, and 0.08 ± 0.02 s for smoke-exposed rats, respectively. The septal thicknesses (d) of healthy versus smoke-exposed rats were 12.03 ± 1.51 μm versus 16.28 ± 1.77 μm , 12.15 ± 1.29 μm versus 16.24 ± 1.39 μm , and 12.01 ± 1.37 μm versus 16.22 ± 1.67 μm for the SB measurement, MB measurement and average of SB measurements, respectively. The extracted parameters from three different datasets were almost the same for the same rat, and all three datasets distinguished the differences in healthy and smoke-exposed rats. The MOXE fitting results for healthy and smoke-exposed rats are shown in figure 5. Pathological changes characterized by greater alveolar

Table 1. The values of the parameters obtained from the SB and MB measurements^a.

| | δ/d | | $T(s)$ | | H | | $tx(s)$ | | $d(\mu m)$ | | $\delta(\mu m)$ | | $SVR = 2b/\lambda^d(\text{cm}^{-1})$ | | Hct | |
|------------------------------------|------------|----------|----------|----------|----------|----------|----------|----------|------------|----------|-----------------|----------|--------------------------------------|----------|----------|----------|
| | SB meas. | MB meas. | SB meas. | MB meas. | SB meas. | MB meas. | SB meas. | MB meas. | SB meas. | MB meas. | SB meas. | MB meas. | SB meas. | MB meas. | SB meas. | MB meas. |
| Mean | 0.15 | 0.15 | 0.05 | 0.05 | 0.58 | 0.60 | 0.44 | 0.43 | 12.03 | 12.14 | 1.78 | 1.83 | 41.44 | 42.46 | 0.40 | 0.42 |
| SD | 0.02 | 0.02 | 0.01 | 0.01 | 0.03 | 0.03 | 0.09 | 0.07 | 1.51 | 1.29 | 0.23 | 0.25 | 7.52 | 6.43 | 0.03 | 0.03 |
| Cronbach's α | 0.92 | | 0.91 | | 0.90 | | 0.88 | | 0.90 | | 0.86 | | 0.98 | | 0.91 | |
| Intraclass correlation coefficient | 0.85 | | 0.83 | | 0.82 | | 0.79 | | 0.81 | | 0.75 | | 0.96 | | 0.83 | |
| Pearson correlation coefficient | 0.85 | | 0.84 | | 0.84 | | 0.84 | | 0.82 | | 0.75 | | 0.97 | | 0.84 | |

^a Mean values and standard deviation of the δ/d , T , fraction of RBC xenon in blood (η), tx , d , δ SVR and Hct obtained from the SB and MB measurements. Cronbach's α coefficients, intraclass correlation coefficients and Pearson correlation coefficients between these two measurements were also calculated.



septal thickness and enlarged mean linear intercepts were confirmed by the pathological conditions of the histological sections.

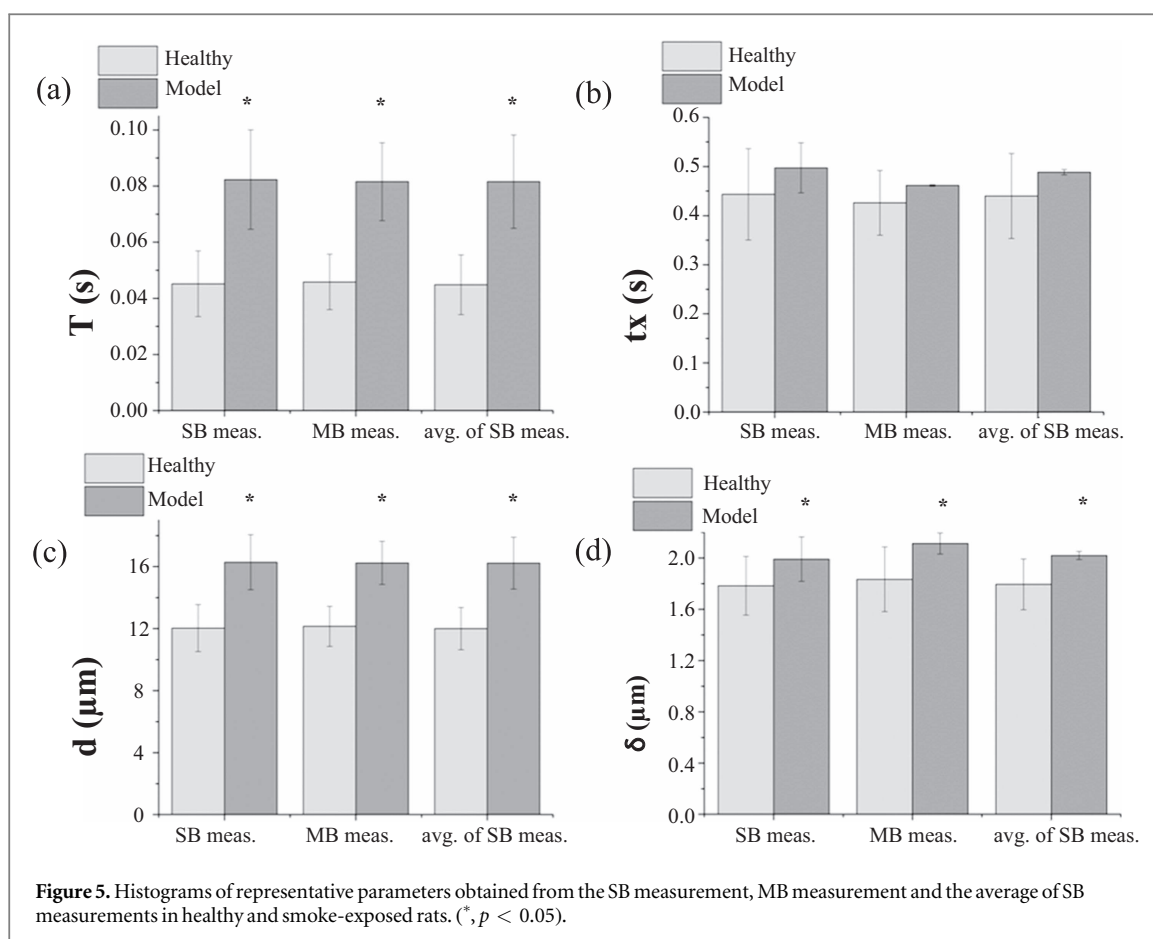
4. Discussion

CSSR has played an important role in the study of the gas exchange function and measurement of the changes in pulmonary structure and function caused by diseases such as COPD, fibrosis, and asthma in both humans and animals (Månsson *et al* 2003, Qing *et al* 2014, Stewart *et al* 2014, Li *et al* 2015). MOXE was used to evaluate the influence of the RBC xenon signal oscillation caused by the cardiac cycle on the fitting results of CSSR data in this study.

The rhythmic pulsation of the xenon signal was assumed to be reduced or even nullified by averaging the CSSR data acquired 8 times. This assumption is reasonable because the acquisitions were random and did not depend on the heartbeat. In most animal studies, the dissolved xenon signal was usually averaged to increase the signal to noise ratio, while the signal was usually acquired without averaging in human experiments (Kaushik *et al* 2014, Qing *et al* 2014). To evaluate the influence of the oscillations caused by the cardiac cycle, the CSSR data with and without signal fluctuation due to the heartbeat were acquired by

using SB and MB measurements, respectively. The SB measurement, completed within a breathhold, economizes hyperpolarized xenon and requires good signal strength of polarized Xe. The requirements for the signal strength in the MB measurement are not as strict as for the SB measurement because of the averaging. However, more breaths are needed for the MB measurement, and the consumption of hyperpolarized xenon in each experiment increases. In addition, in comparison with the SB measurement in which all signals are acquired once and without accumulation, the data are collected in different breaths for the MB measurement, and a risk of changing acquisition conditions for each breath during the experiments is present.

The data obtained from the SB measurement in which all of the signals were acquired once and without accumulation were deemed to contain oscillation caused by the cardiac cycle. However, for the MB measurement, each data point was acquired in a single breathhold with an accumulation of eight and served as the reference data without oscillation. The physiological parameters extracted from both acquisition modes showed good consistency, and the differences between each parameter extracted from the CSSR data were all below 5% between the acquisition modes, which were demonstrated by Cronbach's α



coefficients and intraclass correlation coefficients. These results indicated that the signal oscillations caused by the cardiac cycle had little or even no effect on the pulmonary physiological parameters derived from the CSSR data in rats. This was mostly because the exchange time was varied from 2 to 1000 ms non-periodically at different intervals in this study, and the oscillations seemed to have a random effect on each signal and were difficult to distinguish. The time elapsed between the two types of measurement is about 1 min, and the physiology remains almost constant. The quantities measured are intensive quantities and not extensive, therefore minimal differences were observed between the SB and MB methods. The other important reason was that the acquisition time for each spectrum was approximately 40 ms. The signal itself reflects the signals during the acquiring time, and this reduced the oscillation of the signal amplitude.

The Bland–Altman plots showed that nearly all of the MOXE-derived parameters were within the limits of agreement. Although a few parameters were out of the limits of agreement, the results from healthy and smoke-exposed rats showed significant differences in T , d , δ and SVR. The results showed that the pulmonary microstructure fitting from the data acquired by both methods can distinguish rats with lung disease from healthy rats, although some differences exist in the fitting results between the SB and MB measurements.

In this study, enriched xenon (85% ^{129}Xe) was used to improve the SNR of the dissolved xenon signal for the SB measurement to eliminate a possible fitting error caused by a weak signal. The abundance of ^{129}Xe used in this study was three-fold greater than that in the naturally abundant xenon, which means the signal in this study is almost the same as that acquired using naturally abundant xenon with an average of 9. The RBC xenon signal is larger than that in the TP in most rats when the exchange time is great enough (generally an exchange time longer than 500 ms), mostly because hyperpolarized ^{129}Xe dissolved in RBCs flowed from the lungs in blood, arrived at the blood vessels and capillaries in muscle, and then into the heart. The RBC xenon signal was acquired as a global evaluation, and the signal was the summation of RBC xenon in blood of the lungs and heart, which cannot be distinguished. Another limitation of this study is that the experiments and comparisons were conducted on rats, and whether they can be applied in humans requires further study.

5. Conclusion

In this study, the effects of the fluctuation in the RBC xenon signal caused by the heartbeat on the physiological parameters extracted from MOXE were evaluated in healthy and smoke-exposed rats. The results

indicated that the physiological parameters derived from dissolved xenon dynamics in the lung using both acquisition modes were not significantly different, and the data acquired using both acquisition modes could be used to evaluate changes in the pulmonary structure and function in the smoke-exposed rats. The SB measurement of CSSR in rats economized hyperpolarized Xe, and the CSSR data were acquired within a single breathhold. The consistency between the SB and MB measurements indicated that, although the effect of the varying blood flow velocity was included, the SB measurement would not cause an error in the microstructure fitted with MOXE. The SB measurement in animals has more advantages over the MB measurement if the polarization of the xenon is high enough, which is the recommended acquisition method. Combining ECG signals with CSSR measurements might provide new insights into the dynamics of gas uptake not only in pulmonary function but also in heart function.

Acknowledgments

This work was supported by the National Natural Science Foundation of China (81227902) and National Program for Support of Eminent Professionals (National Program for Support of Top-notch Young Professionals).

References

- Abdeen N, Cross A, Cron G, White S, Rand T, Miller D and Santyr G 2006 Measurement of xenon diffusing capacity in the rat lung by hyperpolarized ^{129}Xe MRI and dynamic spectroscopy in a single breath-hold *Magn. Reson. Med.* **56** 255–64
- Chang Y V 2013 MOXE: a model of gas exchange for hyperpolarized ^{129}Xe magnetic resonance of the lung *Magn. Reson. Med.* **69** 884–90
- Chen B T, Brau A and Johnson G A 2003 Measurement of regional lung function in rats using hyperpolarized ^3He dynamic MRI *Magn. Reson. Med.* **49** 78–88
- Cleveland Z I, Möller H E, Hedlund L W, Nouls J C, Freeman M S, Qi Y and Driehuys B 2012 *In vivo* MR imaging of pulmonary perfusion and gas exchange in rats via continuous extracorporeal infusion of hyperpolarized ^{129}Xe *PLoS One* **7** e31306
- Dregely I, Mugler J P, Ruset I C, Altes T A, Mata J F, Miller G W, Ketel J, Ketel S, Distelbrink J and Hersman F 2011 Hyperpolarized xenon-129 gas-exchange imaging of lung microstructure: first case studies in subjects with obstructive lung disease *J. Magn. Reson. Imaging* **33** 1052–62
- Dregely I, Ruset I C, Mata J F, Ketel J, Ketel S, Distelbrink J, Altes T A, Mugler J P, Wilson Miller G and William Hersman F 2012 Multiple-exchange-time xenon polarization transfer contrast (MXTC) MRI: initial results in animals and healthy volunteers *Magn. Reson. Med.* **67** 943–53
- Driehuys B, Cofer G P, Pollaro J, Mackel J B, Hedlund L W and Johnson G A 2006 Imaging alveolar–capillary gas transfer using hyperpolarized ^{129}Xe MRI *Proc. Natl Acad. Sci. USA* **103** 18278–83
- Driehuys B, Möller H E, Cleveland Z I, Pollaro J and Hedlund L W 2009 Pulmonary perfusion and xenon gas exchange in rats: MR imaging with intravenous injection of hyperpolarized ^{129}Xe *Radiology* **252** 386–93
- Driehuys B, Martinez-Jimenez S, Cleveland Z I, Metz G M, Beaver D M, Nouls J C, Kaushik S S, Firszt R, Willis C and Kelly K T 2012 Chronic obstructive pulmonary disease: safety and tolerability of hyperpolarized ^{129}Xe MR imaging in healthy volunteers and patients *Radiology* **262** 279–89
- Fox M S, Ouriadov A, Thind K, Hegarty E, Wong E, Hope A and Santyr G E 2014 Detection of radiation induced lung injury in rats using dynamic hyperpolarized ^{129}Xe magnetic resonance spectroscopy *Med. Phys.* **41** 072302
- Imai H, Kimura A, Iguchi S, Hori Y, Masuda S and Fujiwara H 2010 Noninvasive detection of pulmonary tissue destruction in a mouse model of emphysema using hyperpolarized ^{129}Xe MRS under spontaneous respiration *Magn. Reson. Med.* **64** 929–38
- Kaushik S S, Freeman M S, Yoon S W, Liljeroth M G, Stiles J V, Roos J E, Foster W S M, Rackley C R, McAdams H P and Driehuys B 2014 Measuring diffusion limitation with a perfusion-limited gas-hyperpolarized ^{129}Xe gas-transfer spectroscopy in patients with idiopathic pulmonary fibrosis *J. Appl. Physiol.* **117** 577–85
- Ladefoged J and Andersen A 1967 Solubility of xenon-133 at 37 C in water, saline, olive oil, liquid paraffin, solutions of albumin, and blood *Phys. Med. Biol.* **12** 353
- Li H, Zhang Z, Zhao X, Sun X, Ye C and Zhou X 2015 Quantitative evaluation of radiation-induced lung injury with hyperpolarized xenon magnetic resonance *Magn. Reson. Med.* **76** 408–16
- Månsson S, Wolber J, Driehuys B, Wollmer P and Golman K 2003 Characterization of diffusing capacity and perfusion of the rat lung in a lipopolysaccharide disease model using hyperpolarized ^{129}Xe *Magn. Reson. Med.* **50** 1170–9
- Marshall H, Parra-Robles J, Hartley R, Kay R and Vos W 2014 A method for quantitative analysis of regional lung ventilation using deformable image registration of CT and hybrid hyperpolarized gas/ ^1H MRI *Phys. Med. Biol.* **59** 7267
- Mugler J P and Altes T A 2013 Hyperpolarized ^{129}Xe MRI of the human lung *J. Magn. Reson. Imaging* **37** 313–31
- Mugler J P, Altes T A, Ruset I C, Dregely I M, Mata J F, Miller G W, Ketel S, Ketel J, Hersman F W and Ruppert K 2010 Simultaneous magnetic resonance imaging of ventilation distribution and gas uptake in the human lung using hyperpolarized xenon-129 *Proc. Natl Acad. Sci. USA* **107** 21707–12
- Muradyan I, Butler J P, Dabaghyan M, Hrovat M, Dregely I, Ruset I, Topulos G P, Frederick E, Hatabu H and Hersman W F 2013 Single-breath xenon polarization transfer contrast (SB-XTC): implementation and initial results in healthy humans *J. Magn. Reson. Imaging* **37** 457–70
- Nouls J, Fanarjian M, Hedlund L and Driehuys B 2011 A constant-volume ventilator and gas recapture system for hyperpolarized gas MRI of mouse and rat lungs *Concepts Magn. Reson. B* **39** 78–88
- Norquay G, Leung G, Stewart N J, Wolber J and Wild J M 2016 ^{129}Xe chemical shift in human blood and pulmonary blood oxygenation measurement in humans using hyperpolarized ^{129}Xe NMR *Magn. Reson. Med.* accepted (doi:10.1002/mrm.26225)
- Patz S, Muradian I, Hrovat M I, Ruset I C, Topulos G, Covrig S D, Frederick E, Hatabu H, Hersman F and Butler J P 2008 Human pulmonary imaging and spectroscopy with hyperpolarized ^{129}Xe at 0.2 T *Acad. Radiol.* **15** 713–27
- Patz S, Muradyan I, Hrovat M I, Dabaghyan M, Washko G R, Hatabu H and Butler J P 2011 Diffusion of hyperpolarized ^{129}Xe in the lung: a simplified model of ^{129}Xe septal uptake and experimental results *New J. Phys.* **13** 015009
- Peterson E T, Dai J, Holmes J H and Fain S B 2011 Measurement of lung airways in three dimensions using hyperpolarized helium-3 MRI *Phys. Med. Biol.* **56** 3107
- Qing K, Mugler J P, Altes T A, Jiang Y, Mata J F, Miller G W, Ruset I C, Hersman F W and Ruppert K 2014 Assessment of lung function in asthma and COPD using hyperpolarized ^{129}Xe chemical shift saturation recovery spectroscopy and dissolved-phase MRI NMR *Biomed.* **27** 1490–501

- Ruppert K, Altes T A, Mata J F, Ruset I C, Hersman F W and Mugler J P 2015 Detecting pulmonary capillary blood pulsations using hyperpolarized xenon-129 chemical shift saturation recovery (CSSR) MR spectroscopy *Magn. Reson. Med.* **75** 1771–80
- Ruppert K, Brookeman J R, Hagspiel K D and Mugler J P 2000 Probing lung physiology with xenon polarization transfer contrast (XTC) *Magn. Reson. Med.* **44** 349–57
- Sakai K, Bilek A M, Oteiza E, Walsworth R L, Balamore D, Jolesz F A and Albert M S 1996 Temporal dynamics of hyperpolarized ^{129}Xe resonances in living rats *J. Magn. Reson. Imaging Ser. B* **111** 300–4
- Sodickson A, Baeyens P F, Andriole K P, Prevedello L M, Nawfel R D, Hanson R and Khorasani R 2009 Recurrent CT, cumulative radiation exposure, and associated radiation-induced cancer risks from CT of adults *Radiology* **251** 175–84
- Stewart N J, Leung G, Norquay G, Marshall H, Parra-Robles J, Murphy P S, Schulte R F, Elliot C, Condliffe R and Griffiths P D 2014 Experimental validation of the hyperpolarized ^{129}Xe chemical shift saturation recovery technique in healthy volunteers and subjects with interstitial lung disease *Magn. Reson. Med.* **74** 196–207
- Zhou X 2011 *In vivo NMR Imaging: Methods and Protocols* (New Jersey: Humana Press) pp 189–204
- Zhu F, Qiu X, Wang J, Jin Y, Sun Y, Lv T and Xia Z 2012 A rat model of smoke inhalation injury *Inhalation Toxicol.* **24** 356–64